J|A|C|S
ARTICLES
Published on Web 03/23/2006

Changing the Ligation of the Distal [4Fe4S] Cluster in NiFe Hydrogenase Impairs Inter- and Intramolecular Electron Transfers

Sébastien Dementin,[†] Valérie Belle,[†] Patrick Bertrand,[†] Bruno Guigliarelli,[†] Géraldine Adryanczyk-Perrier,[†] Antonio L. De Lacey,[‡] Victor M. Fernandez,[‡] Marc Rousset,[†] and Christophe Léger*[,†]

Contribution from the Laboratoire de Bioénergétique et Ingénierie des Protéines, CNRS UPR 9036, IBSM and Université de Provence, 31 chemin Joseph Aiguier, 13402 Marseille Cédex 20, France, and Instituto de Catalisis, CSIC, C/Marie Curie 2, Cantoblanco, 28049 Madrid, Spain

Received January 24, 2006; E-mail: christophe.leger@ibsm.cnrs-mrs.fr

Abstract: In NiFe hydrogenases, electrons are transferred from the active site to the redox partner via a chain of three Iron−Sulfur clusters, and the surface-exposed [4Fe4S] cluster has an unusual $His(Cys)_3$ ligation. When this Histidine (H184 in *Desulfovibrio fructosovorans*) is changed into a cysteine or a glycine, a distal cubane is still assembled but the oxidative activity of the mutants is only 1.5 and 3% of that of the WT, respectively. We compared the activities of the WT and engineered enzymes for H_2 oxidation, H^+ reduction and H/D exchange, under various conditions: (i) either with the enzyme directly adsorbed onto an electrode or using soluble redox partners, and (ii) in the presence of exogenous ligands whose binding to the exposed Fe of H184G was expected to modulate the properties of the distal cluster. Protein film voltammetry proved particularly useful to unravel the effects of the mutations on inter and intramolecular electron transfer (ET). We demonstrate that changing the coordination of the distal cluster has no effect on cluster assembly, protein stability, active-site chemistry and proton transfer; however, it slows down the first-order rates of ET to and from the cluster. All-sulfur coordination is actually detrimental to ET, and intramolecular (uphill) ET is rate determining in the glycine variant. This demonstrates that although [4Fe4S] clusters are robust chemical constructs, the direct protein ligands play an essential role in imparting their ability to transfer electrons.

Introduction

Hydrogenases are present in some eukaryotes and in virtually all bacteria.[1−3] These enzymes catalyze a reaction that is essential in the energetics of these organisms and has promising technological applications:[4] the reversible oxidation of H_2. The hydrogenases that contain iron−sulfur (FeS) clusters[5] have been classified according to whether their active site is a dinuclear cluster of nickel and iron[7] or iron only.[8] In both cases, the electrons produced upon H_2 oxidation at the active site are transferred to the redox partner via a chain of closely spaced FeS clusters, one of which is exposed at the surface of the enzyme. Similar redox chains occur in many respiratory enzymes, including mitochondrial complexes I[9,10] and II,[11] but there have been no measurements of electron transfer (ET) rates between FeS clusters in these enzymes;[12] this is a direct consequence of two experimental limitations: FeS clusters lack the well-resolved UV−vis features that are required for time-resolved spectroscopic studies, and ET can be difficult to trigger in non-light-driven enzymes.[16] Nevertheless, it is generally believed that intramolecular ET is fast with respect to the active site chemistry, so that it does not limit turnover,[17] and NiFe hydrogenases are actually cited as a paradigm in this respect.[18]

Vignais and co-workers have classified NiFe hydrogenases on the basis of sequence homologies.[1] In group 1 NiFe

[†] Laboratoire de Bioénergétique et Ingénierie des Protéines, CNRS.
[‡] Instituto de Catalisis, CSIC.

(1) Vignais, P. M.; Billoud, B.; Meyer, J. *FEMS Microbiol. Rev.* **2001**, *25*, 455−501.
(2) Cammack, R.; Frey, M.; Robson, R.; Eds. *Hydrogen as a Fuel, Learning from Nature*; Taylor and Francis: London and New York, 2001.
(3) Armstong, F. A. *Curr. Op. Chem. Biol.* **2004**, *8*, 133−140.
(4) Vincent, K. A.; Cracknell, J. A.; Lenz, O.; Zebger, I.; Friedrich, B.; Armstrong, F. A. *Proc. Natl. Acad. Sci., U.S.A.* **2005**, *102*, 16951−16954.
(5) A third class of hydrogenase, formerly known as "metal-free" is characterized by having no FeS clusters and a single Fe atom at the active site. See ref 6.
(6) Shima, S.; Lyon, E. J., Thauer, R. K.; Mienert B.; Bill E. *J. Am. Chem. Soc.* **2005**, *127*, 10430−10435.
(7) Volbeda, A.; Charon, M. H.; Piras, C.; Hatchikian, E. C.; Frey, M.; Fontecilla-Camps, J. C. *Nature* **1995**, *373*, 580−587.
(8) Peters, J. W.; Lanzilotta, W. N.; Lemon, B. J.; Seefeldt, L. C. *Science* **1998**, *282*, 1853−1858.
(9) Hinchliffe, P.; Sazanov, L. A. *Science* **2005**, *309*, 771−774.
(10) Sazanov, L. A.; Hinchliffe, P. *Science* **2006**, *311*, 1430−1436.
(11) Yankovskaya, V.; Horsefield, R.; Törnroth, S.; Luna-Chavez, C.; Miyoshi, H.; Léger, C.; Byrne, B.; Cecchini, G.; Iwata, S. *Science* **2003**, *299*, 700−704.
(12) Only in selected ferredoxins could NMR be used to measure intramolecular ET rates between [4Fe4S] clusters. See refs 13−15.
(13) Kyritsis, P.; Huber, J. G.; Quinkal, I.; Gaillard, J.; Moulis, J. M. *Biochemistry* **1997**, *36*, 7839−7846.
(14) Kummerle, R.; Kyritsis, P.; Gaillard, J.; Moulis, J.-M. *J. Inorg. Biochem.* **2000**, *79*, 83−91.
(15) Kummerle, R.; Gaillard, J.; Kyritsis, P.; Moulis, J.-M. *J. Biol. Inorg. Chem.* **2001**, *6*, 446−451.
(16) Léger, C.; Lederer, F.; Guigliarelli, B.; Bertrand, P. *J. Am. Chem. Soc.* **2006**, *128*, 180−187.

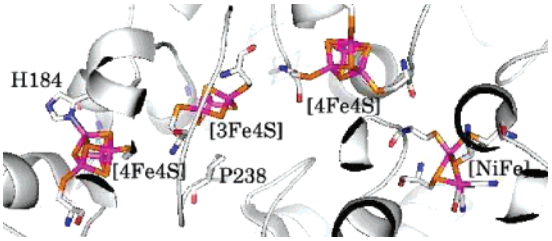

Figure 1. Biological wire which links the active site to the redox partner in NiFe hydrogenases (PDB file 1YQW).[19] In the enzyme from *D. fructosovorans*, the reduction potentials of the centers are ∼−340 mV vs SHE for the two [4Fe4S] clusters and +65 mV for the [3Fe4S] cluster.[20] In the enzyme from *D. gigas*, the reported values are −290 and −340 mV for the two [4Fe4S] clusters, and −70 mV for the medial cluster.[21]

hydrogenases, defined as respiratory (i.e., H_2-uptake) enzymes, the redox chain that mediates the electron transfer between the active site and the redox partner consists of a proximal (to the active site) [4Fe4S] cluster, a medial [3Fe4S] and a distal [4Fe4S] (Figure 1).

The activity of NiFe hydrogenases can be quantified in several ways that each probe a distinct set of steps in the catalytic cycle.[2] The rates of hydrogen oxidation and proton reduction can be measured using either artificial redox dyes or the natural partner cytochrome c_3 as electron acceptors or donors; this reaction involves intermolecular ET at the exposed FeS site, intramolecular ET along the redox chain, proton transfers and hydrogen activation. In contrast, the activity for the "isotope exchange" reaction ($D_2 + H^+ \rightleftharpoons HD + D^+$) does not involve ET.

In the H_2 oxidation process, the rate-limiting step is the oxidation of the enzyme by the redox partner (i.e., intermolecular ET). This is obvious from experiments where the rate of H_2 consumption is highly dependent on the nature of the electron acceptor[22−24] and some correlation was observed between the turnover rate and the reduction potential of the redox dye that accepts the electrons in the assay.[23] Consistently, when the enzyme is adsorbed on a "friendly" electrode poised at high potential, H_2 oxidation is at least an order of magnitude faster than with any soluble electron acceptor.[3,24]

The relatively high reduction potential of the medial [3Fe4S] cluster makes intramolecular ET to the distal center very endergonic. Yet the P238C mutant, which has a nearly isopotential redox chain with a medial [4Fe4S] cluster, is just as active as the WT enzyme in solution assays of H_2 oxidation:[20] since intermolecular ET limits the turnover rate, speeding up intramolecular ET does not increase the overall activity.

The distal cluster is unusual in that one of the Fe atoms is coordinated by the N atom of a histidine which is exposed at the surface of the protein.[7] This type of coordination is rare: it was also demonstrated by X-ray crystallography only in some enzymes from the DMSO-reductase family, including the membrane-bound nitrate reductase from *Escherichia coli* (*Ec*),[25] in clostridial-type Fe-only hydrogenases,[8] and in respiratory Complex I.[10] Site-directed mutagenesis experiments have shown that the conserved histidine ligand is required for activity, but its potential function in tuning the properties of the cluster has not been defined further. The His to Cys variant of *Clostridium acetobutylicum* Fe-only hydrogenase was not produced in quantities large enough for structural and thermodynamic studies (M. Demuez, P. Soucaille, and L. Girbal, unpublished results). The activity of the His to Cys mutant of {\em Ec} nitrate reductase is 0.5% of that of the WT enzyme.[27]

The histidinyl ligation of [4Fe4S] clusters seems to have no major effect on their redox properties. In NiFe hydrogenases, the two cubanes appear to have approximately the same reduction potential (∼−350 mV) despite their distinct coordinations,[20,21] and this also seems to be the case in Fe-only hydrogenases. Regarding *Ec* nitrate reductase, Rothery and coworkers have shown that the histidinyl cluster has moderately high reduction potential (−55mV);[28] the properties of the engineered all-cysteinyl cluster[27] have not been reported yet. The attempts to use site-directed mutagenesis to engineer histidine ligands to [4Fe4S] clusters were mostly unsuccessful (see ref 29 and refs therein): often, either the cluster is converted to a [3Fe4S] form or the protein is not produced. Only in the DNA-repair enzyme MutY could a histidinyl ligation of a [4Fe4S] cluster be engineered:[30,31] one peculiar Cys/His mutation, which leaves the activity unchanged, decreases the reduction potential of the DNA-bound, $[4Fe4S]^{3+/2+}$ couple.[32] However, the 70 mV negative shift is small compared, for example, to the difference between the reduction potentials of Rieske-type and all-cysteinyl [2Fe2S] clusters.

Over the last years, we have designed molecular biology procedures to clone and express in *D. fructosovorans* (*Df*) a Strep-tag construct of NiFe-hydrogenase. This allows us to purify mutant enzymes in amounts usually compatible with material-demanding techniques.[20,33−35] To study the function of the histidine that ligates the distal [4Fe4S] cluster in *Df* NiFe hydrogenase (H184), we have exchanged it for a cysteine or a glycine. By comparing the properties of the WT and variant hydrogenases, we demonstrate the essential function of this residue in increasing the rates of inter and intramolecular ET to and from the distal cluster.

(17) Page, C. C.; Moser, C. C.; Dutton, P. L. *Curr. Op. Chem. Biol.* **2003**, *7*, 551−556.
(18) Page, C. C.; Moser, C. C.; Chen, X.; Dutton, P. L. *Nature* **1999**, *402*, 47−52.
(19) Volbeda, A.; Martin, L.; Cavazza, C.; Matho, M.; Faber, B. W.; Roseboom, W.; Albracht, S. P. J.; Garcin, E.; Rousset, M.; Fontecilla-Camps, J. C. *J. Biol. Inorg. Chem.* **2005**, *10*, 239−249, *Erratum* **2005**, *10*, 591.
(20) Rousset, M.; Montet, Y.; Guigliarelli, B.; Forget, N.; Asso, M.; Bertrand, P.; Fontecilla-Camps, J. C.; Hatchikian, E. C. *Proc. Natl. Acad. Sci., U.S.A.* **1998**, *95*, 11625−11630.
(21) Teixeira, M.; Moura, I.; Xavier, A. V.; Moura, J. J. G.; Legall, J.; Dervartanian, D. V.; Peck, H. D.; Huynh, B. H. *J. Biol. Chem.* **1989**, *264*, 16435−16450.
(22) Bertrand, P.; Dole, F.; Asso, M.; Guigliarelli, B. *J. Biol. Inorg. Chem.* **2000**, *5*, 682−691.
(23) Delacey, A. L.; Santamaria, E.; Hatchikian, E. C.; Fernandez, V. M. *Biochim. Biophys. Acta* **2000**, *1481*, 371−380.
(24) Pershad, H. R.; Duff, J. L. C.; Heering, H. A.; Duin, E. C.; Albracht, S. P. J.; Armstrong, F. A. *Biochemistry* **1999**, *38*, 8992−8999.
(25) Bertero, M. G.; Rothery, R. A.; Palak, M.; Hou, C.; Lim, D.; Blasco, F.; Weiner, J. H.; Strynadka, N. C. J. *Nat. Struct. Biol.* **2003**, *10*, 681−687.
(26) Albracht, S. P.; Mariette, A.; de Jong, P. *Biochim. Biophys. Acta* **1998**, *1318*, 92−106.
(27) Magalon, A.; Asso, M.; Guigliarelli, B.; Rothery, R. A.; Bertrand, P.; Giordano, G.; Blasco, F. *Biochemistry* **1998**, *37*, 7363−7370.
(28) Rothery, R. A.; Bertero, M. G.; Cammack, R.; Palak, M.; Blasco, F.; Strynadka, N. C. J.; Weiner, J. H. *Biochemistry* **2004**, *43*, 5324−5333.
(29) Moulis, J.-M.; Davasse, V.; Golinelli, M.-P.; Meyer, J.; Quinkal, I. *J. Biol. Inorg. Chem.* **1996**, *1*, 2−14.
(30) Golinelli, M. P.; Chmiel, N. H.; David, S. S. *Biochemistry* **1999**, *38*, 6997−7007.
(31) Messick, T. E.; Chmiel, N. H.; Golinelli, M.-P.; Langer, M. R.; Joshua-Tor, L.; David, S. S. *Biochemistry* **2002**, *41*, 3931−3942.
(32) Boon, E. M.; Livingston, A. L.; Chmiel, N. H.; David, S. S.; Barton, J. K. *Proc. Natl. Acad. Sci., U.S.A.* **2003**, *100*, 12543−12547.
(33) DeLacey, A. L.; Fernandez, V. M.; Rousset, M.; Cavazza, C.; Hatchikian, E. C. *J. Biol. Inorg. Chem.* **2003**, *8*, 129−134.
(34) Dementin, S.; Burlat, B.; DeLacey, A. L.; Pardo, A.; Adryanczyk-Perrier, G.; Guigliarelli, B.; Fernandez, V. M.; Rousset, M. *J. Biol. Chem.* **2004**, *279*, 10508−10513.
(35) DeLacey, A. L.; Fernandez, V. M.; Rousset, M. *Coord. Chem. Rev.* **2005**, *249*, 1596−1608.

Experimental Procedures

Bacterial Strains, Plasmids and Growth Conditions. *Escherichia coli* strain DH5α, F$^-$, *end*A1, *hsd*R17 (r_K^- m_K^+), *sup*E44, *thi*$^{-1}$, λ$^-$, *rec*A1, *gyr*A96, *rel*A1, Δ(*arg*F$^-$ *lac*ZYA) U169, ϕ80d*lac*ZΔM15 was used as a host in the cloning of recombinant plasmids. The bacterium was routinely grown at 37 °C in LB medium. Ampicillin at 100 μg/mL or gentamycin at 20 μg/mL was added when cells harbored pUC18 or pBGF4 derivatives, respectively. The pBGF4 plasmid reporting the gentamycin resistance gene,[36] was used to carry the [NiFe] hydrogenase operon from *Df*.[20] The strain *Df* MR400 [*hyn*::*npt* Δ*hynABC*] carrying a deletion in the [NiFe] hydrogenase operon[37] was grown anaerobically at 37 °C in SOS medium.[36] Large culture volumes were performed as described previously.[20] Kanamycin at 50 μg/mL was present routinely, and 20 μg/L gentamycin was added only when cells harbored the plasmid pBGF4.

Site-Directed Mutagenesis. The QuikChange TM XL site-directed mutagenesis kit (Stratagene, Amsterdam, The Netherlands) was used to generate point mutations in the small subunit *hynA*. The PstI−HindIII fragment from pBGF4 was subcloned in pUC18 to generate the template that was used in mutagenesis experiments. After mutagenesis, the PstI−HindIII fragment was fully sequenced and inserted in the PstI−HindIII digested pBGF4. The recombinant plasmid was introduced into *Df* strain MR400 by electrotransformation.[36]

Protein Purification. The Strep tag II sequence (IBA Gmbh, Göttingen, Germany) was introduced in the hydrogenase gene, and the tagged protein was purified on a Strep-Tactin(R) column (IBA Gmbh), as described previously.[34] An additional purification step using a HiLoad TM 26/60 Superdex TM 200 prep grade column (Amersham Biosciences, Uppsala, Sweden) was performed. The purification yield was about 0.7 mg of pure hydrogenase per liter of culture for both the WT and H184C enzymes, but only 5 μg/L for the H184G mutant. The untagged *Df* NiFe hydrogenase was prepared as described in ref 20.

Redox Titrations and Spectroscopies. The redox titration of the H184C mutant was carried out at 25 °C in a specially designed anaerobic cell containing a solution of purified enzyme (34 μM) in 50 mM HEPES buffer at pH 8 under an argon atmosphere. Redox potentials were measured with a combined Pt−Ag/AgCl/KCl (3 M) microelectrode, in the presence of a cocktail of mediators consisting of 15 μM in each of 1,2 naphthoquinone, methylene blue, resorufine, indigo carmine, phenosafranine, neutral red, and methyl viologen. The titration was conducted by stepwise additions of small amounts of sodium dithionite solution (20 mM in oxygen-free HEPES buffer). All potentials are quoted against the standard hydrogen electrode (SHE).

For the H184G mutant only 150 μL of enzyme at 10 μM was available, precluding a redox titration of the protein. The reduced state was obtained by adding in the EPR tube an excess of dithionite (1:200) under anaerobic conditions.

The EPR spectra were recorded on a Bruker ELEXSYS E500 spectrometer fitted with an Oxford Instruments ESR 900 helium flow cryostat. For spin quantitation, the double integration of the signal recorded under non saturating conditions was compared with that given by a $CuSO_4$ standard at the same temperature.

The metal content of the variants was measured using ICP-MS analysis (spectrometer HP 4500, calibrated using external standards).

Solution Assays. Unless otherwise stated, the purified enzymes were activated for 1h at 37 °C in an anaerobic cuvette containing 500 μL of 100 mM Tris/HCl buffer at pH 8 with 0.2 mM methyl viologen (MV). Before adding the enzyme, oxygen was removed under vacuum, the cuvette was flushed with H_2 and 1 μL of a 1M dithionite solution was added to eliminate the residual oxygen.

H_2-oxidation activity was measured at 30 °C in a UV cuvette containing 1 mL of buffer Tris/HCl 100 mM at pH 8 with 0.5−500 mM MV and the exogenous ligand as required. Oxygen was removed under vacuum, the cuvette was flushed with H_2, and dithionite was added to eliminate the residual oxygen. The reaction was started by the addition of 5−20 μL of stock solution of activated enzyme (30−55 nM), and the rate of MV reduction was measured at 604 nm with a UV 1601 spectrophotometer (Shimadzu). The H_2/methylene blue assay was performed under the same conditions except that 50−100 μM methylene blue (MB) substituted for MV. The reduction of MB was detected at 600 nm.

The assays of H_2-evolution were performed in a thermostated (30 °C) anaerobic vessel connected through a 14 μm Teflon membrane to a mass spectrometer (Masstorr DX 200, VG Quadrupoles Ltd.), and containing 10 mL of buffer (50 mM HEPES, 0.01−1 mM MV, pH 7) flushed with nitrogen until dissolved O_2 was eliminated (this was followed by the decrease of mass-32 signal). Then, 75 μL of 2 M sodium dithionite were injected into the vessel in order to reduce the dye. Finally, 5−20 μL of activated hydrogenase (4.5−6.5 μM) were injected, and the evolution of H_2 was detected as an increase in mass-2 signal. The assays of H^+/D_2 exchange were performed as described in ref 33.

Protein Film Voltammetry. We used the same electrochemical setup and equipment as described in ref 38. The mixed buffer consisted of MES, HEPES, sodium acetate, TAPS, and CHES (5 mM of each component), 1 mM EDTA, and 0.1 M NaCl as supporting electrolyte. The H184G variant of hydrogenase was adsorbed onto a pyrolytic graphite edge electrode by painting the surface with about 0.5 μL of stock solution of enzyme (∼2 μM in 50 mM HEPES.Na, pH 8). To activate the H184G variant, the enzyme-coated electrode was then inserted in the electrochemical cell containing the buffer at pH 7, 40 °C, with 10 mM imidazole, under an atmosphere of H_2, and poised at −560 mV vs SHE for about 1 h. The extent of activation was monitored by taking the electrode potential to −160 mV to measure the H_2 oxidation current. The electrode could then be rinsed and transferred to an imidazole-free solution. Buffered solutions of 1 M imidazole, 1-propanol and 3-mercapto-1-propanol were added to the cell to give the desired final concentrations. Although we observed that imidazole is directly reduced on graphite at potentials below 0V vs SHE at pH 7, the reductive current was small enough not to interfere with the electrochemical measurements.

Origin of Chemicals and Cautions. Imidazole, 1-methyl-imidazole and methylene blue were from Fluka. 1-propanol was from Prolabo. Methyl viologen (caution: toxic and suspected mutagen), and 3-mercaptopropanol (caution: toxic) were from Aldrich. Sodium dithionite was from Merck.

Results

Spectroscopy. To analyze the influence of the H184 mutation on the properties of the metal centers, the two mutants and the WT enzyme were studied by EPR spectroscopy.

In the oxidized state, both mutants exhibited spectra identical with those previously reported for the WT enzyme:[20,34,39] a major Ni-A (g = 2.32, 2.23, 2.01) and a minor Ni−B (g = 2.34, 2.16, 2.01) signals (not shown), and a weakly anisotropic signal centered at g = 2.02, accounting for 1 spin per molecule and arising from the medial $[3Fe4S]^+$ center (Figure 2A). No other signal was detected sweeping from 0 to 600 mT, over the temperature range 6−100 K; this showed that no centers with spin $S > 1/2$ contributed to the spectrum.

(36) Rousset, M.; Casalot, L.; Rapp-Giles, B. J.; Dermoun, Z.; de Philip, P.; Belaich, J. P.; Wall, J. D. *Plasmid* **1998**, *39*, 114−122.
(37) Rousset, M.; Dermoun, Z.; Chippaux, M.; Belaich, J. P. *Mol. Mic.* **1991**, *5*, 1735−1740.
(38) Léger, C.; Dementin, S.; Bertrand, P.; Rousset, M.; Guigliarelli, B. *J. Am. Chem. Soc.* **2004**, *126*, 12162−12172.
(39) Hatchikian, C. E.; Traore, A. S.; Fernandez, V. M.; Cammack, R. *Eur. J. Biochem.* **1990**, *187*, 635−643.

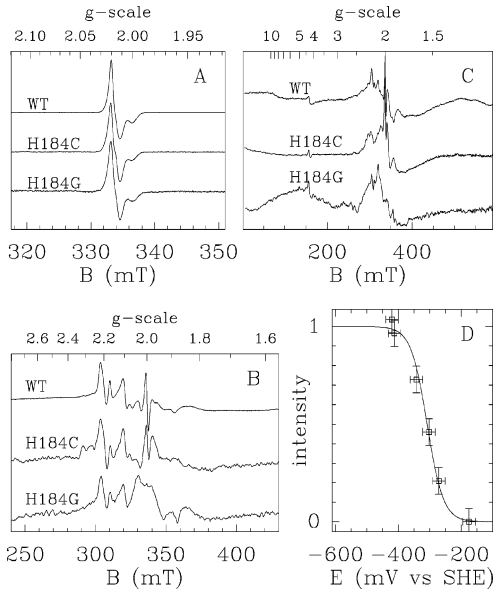

Figure 2. EPR spectra of hydrogenases in the oxidized (Panel A) and reduced (B and C) states. Panel D: potentiometric titration curve of the positive peak around $g = 2.20$ in H184C. Experimental conditions were as follows. Microwave frequency: 9.42 GHz. (A) $T = 15$ K, microwave power $P = 0.1$ mW, modulation amplitude MA = 0.1 mT (WT and H184C) or 0.5 mT (H184G); (B) $T = 6$ K, $P = 10$ mW, MA = 1 mT, $E = -360$ mV (WT) and -340 mV (H184C); (C) $T = 6$ K, $P = 10$ mW, MA = 1 mT (WT) and 2 mT (both mutants), $E = -470$ mV (WT) and -420 mV (H184C). The H184G sample was reduced without potential control (see text).

When the H184C variant was titrated from +150 mV to −420 mV, the spectral changes were very similar to those observed for the WT enzyme. The $[3Fe4S]^+$ signal was no longer visible below ∼−100 mV, and the Ni−A and Ni−B signals decreased progressively and disappeared at about −270 mV. Below −300 mV, these signals were replaced by the usual Ni−C signal ($g = 2.19, 2.14, 2.01$), the amplitude of which exhibited a bell-shaped variation against potential, with a maximum at ≈ −340 mV, as observed in the WT enzyme.[20] At low temperature (6 K), this signal was split by the magnetic interactions with the proximal $[4Fe4S]^+$ center, and showed major features at $g =$ 2.21 and 2.10, as for the WT enzyme[20] (Figure 2B). The minor features observed at lower field result from a small proportion of the active site being in the Ni−L state (compare with Figure 1 in ref 40). In addition, a broad and fast-relaxing signal appeared, which was similar to the broad spectrum observed for the fully reduced WT enzyme,[20] arising from the two $[4Fe4S]^+$ clusters interacting magnetically with the $S = 2$ reduced $[3Fe4S]^0$ cluster (Figure 2C).

Still for the H184C enzyme, a midpoint potential of −310 mV was deduced from the titration of the positive peak in the $g = 2.20$ region (Figure 2D); this value is close to that of −340 mV found for the [4Fe4S] centers in the WT hydrogenase.[20] The comparison of the spin-integration measurements performed in the fully reduced WT enzyme and in the sample of H184C poised at −420 mV indicated that 1.4 [4Fe4S] cluster per molecule is reduced at this potential in the mutant. Since the Ni−C signal was completely in the split form below −340 mV, the proximal [4Fe4S] center was fully reduced in this sample. This implies that a distal [4Fe4S] cluster is present and at least partly reduced. Although its reduction potential could not be determined accurately, it can be concluded that it cannot be more negative than ∼−450 mV. Therefore, all of the FeS clusters are present in the H184C mutant. This was confirmed by ICP-MS elemental analysis which gave an Fe to Ni ratio of 12.7 ± 2. Attempts to determine the crystal structure of this mutant are now being made; the result will indicate whether conformational changes around the distal culster are induced by the substitution.

Table 1: Kinetic Properties of Recombinant *Df* NiFe Hydrogenases, Untagged WT, Strep-tagged WT, and Strep-tagged H184G and H184C Variants in the Presence or Absence of Imidazole (Im)[a]

activity:	H_2-oxidation			exchange	H^+-reduction	
redox partner:	oxidized MV		100 μM MB	none	reduced MV	
	K_m[a]	v_m[b]	v[c]	v[d]	K_m[a]	v_m[b]
WT (no tag)	3.2	630				
WT (Strep-tagged)	9	500	1000	87	0.02	130
WT + 0.1 M Im	7.2	480	780			
H184G	2.2	15	23	74	0.044	96
H184G + 0.1 M Im	2.7	150	180	82		103
H184C	16	8.4	7	70	0.033	61
H184C + 0.1 M Im	14	8.5	5			

[a] The rates are in Units of μmol of gas consumed or produced per min and per mg of enzyme (1 Unit ≈ 1.5 mol per second and per mol of enzyme), and the K_m values are in mM. All relative errors are of the order of 10%. (a) Michaelis constants (relative to the redox partner as indicated). [b]Maximal rates in the assays of H_2 oxidation or production. [c] Rates of H_2-oxidation in the presence of 100 μM oxidized MB (under conditions where the activity is proportional to the concentration of redox partner). [d] Rates of formation of HD in the H^+/D_2 exchange assay. The buffer was 100 mM TRIS at pH 8 for H_2 oxidation and H^+/D_2 exchange, or 50 mM HEPES at pH 7 for H^+ reduction, $T = 30$ °C in all cases

The H184G was not available in high enough amounts to perform a complete titration. The elemental analysis gave an Fe to Ni ratio identical to that in H184C (12 ± 2), showing that a distal cluster was assembled, and the fact that no new [3Fe4S] signal was detected in the oxidized state demonstrates that the glycine mutation has not induced cluster conversion (Figure 2A). In the reduced state, the thin lines of the "Ni−C split" signal in Figure 2B revealed an intact active site, and the broad pattern resulting from the magnetically interacting clusters was essentially identical to that observed for the WT and H184C enzymes ($g = 1.5-1.9$, Figure 2C). The presence of a distal [4Fe4S] cluster in this mutant was also clearly demonstrated by our kinetic data (see below).

Solution Kinetics. The enzymes were assayed for hydrogen oxidation at pH 8, 30 °C, under an atmosphere of H_2, using methyl viologen (MV) as electron acceptor. The comparison of the first two lines in Table 1, shows that engineering a Strep-tag increases 3-fold the Michaelis−Menten constant for MV (despite the fact that we positioned the tag on the side of the enzyme opposite to the distal cubane where the MV interacts) but has only a small effect (−20%) on the rate of H_2 oxidation under saturating conditions.

The data in Table 1 (rows 2, 4 and 6) show that the mutations have only a small effect on the Michaelis constants relative to MV^{2+}, whereas the maximal rates of H_2 oxidation by H184G and H184C are only 3% and 1.7% of that of the WT, respectively. The rates of H_2 oxidation in the presence of 100 μM methylene blue (MB) to accept the electrons are given in Table 1. The high absorbance of oxidized MB made it impossible to perform the assay with greater concentrations of acceptor. In the accessible concentration range, the rate was

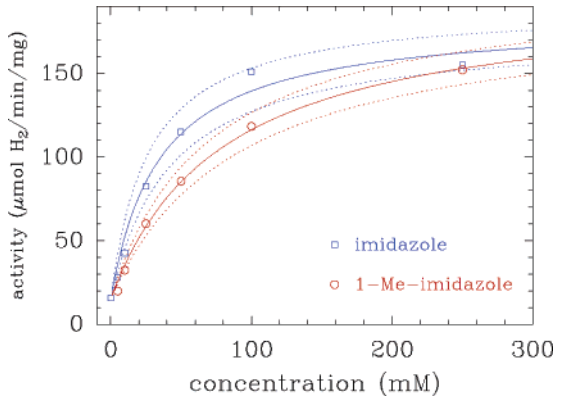

Figure 3. Chemical rescue of H184G hydrogenase: effect on the oxidative activity of imidazole (□) and 1-methyl-imidazole (○). The parameters obtained from the fits to eq 1 are given in the text. pH 8, 30 °C, 50 mM MV, 1 atm of H_2.

proportional to the concentration of MB (data not shown), which demonstrates that the Michaelis constant for MB is greater than 100 μM. Therefore, the H_2/MB rates in Table 1 are far below their maximal values; yet they are significantly higher than when MV accepts the electrons. This confirms that intermolecular ET limits oxidative turnover.[3,22−24]

The effect of the mutations does not depend much on whether MB or MV accepts the electrons in the assay: the His/Gly and His/Cys mutations decrease the activity 45 and 140-fold, respectively, in the H_2/MB assay, compared to 35 and 60-fold in the H_2/MV assay.

The maximal rates of proton reduction by H184G and H184C with MV as electron donor are about 75% and 45% of that of the WT and the mutations have a small effect on the Michaelis constants for $MV^{+\bullet}$ (the differences between the K_m values relative to oxidized versus reduced MV may result, in part, from the charge on the dye being dependent on its redox state). The mutations have a much weaker effect on the rates of H^+ exchange with D_2 than on H_2-oxidation. These observations imply that both mutations leave the active site entirely functional.

Chemical Rescue and Inhibition of H184G in Solution Assays. We repeated the assays in the presence of exogenous ligands which were expected to substitute for the histidine in the H184G variant.

The results of the assays of H^+/D_2 exchange and H_2 oxidation or production with either electron acceptor in the presence of 0.1 M imidazole are collected in Table 1. Exogenous imidazole at 0.1 M has no significant effect on any of the catalytic properties of the WT and H184C enzymes. Regarding the H184G variant, the only significant effect is on its oxidative activity, which increases 10-fold in the presence of imidazole.

Figure 3 shows how the oxidative activity of H184G depends on the concentration of imidazole and 1-methyl-imidazole (methylation is on one of the nitrogen atoms). The changes in turnover number against ligand concentration can be interpreted assuming equilibrium between the free and associated forms of the enzyme. Noting K_d, the dissociation constant between the enzyme and the imidazole derivative, v_0 the activity of the free H184G enzyme and v_∞ the activity of the enzyme bound to the ligand, and provided the concentration of ligand C is greater than the total concentration of enzyme, the activity $v(C)$ reads

$$v(C) = v_0 \frac{1 + \frac{v_\infty C}{v_0 K_d}}{1 + \frac{C}{K_d}} \quad (1)$$

For imidazole, the fit of the data in Figure 3 to eq 1 (with v_0 fixed to 15 Units) gave the values of $K_d = 35 \pm 8$ mM and $v_\infty/v_0 = 12.2 \pm 0.5$. For 1-methyl-imidazole, we obtained $K_d = 80 \pm 10$ mM and $v_\infty/v_0 = 13.1 \pm 0.5$. The dotted lines in Figure 3 illustrate these uncertainties. Control experiments (not shown) were performed to check that neither imidazole (up to 0.25 M) nor 1-methyl-imidazole (up to 0.5 M) have an effect on the activity of the WT and H184C enzymes.

Figure 4 shows how the addition of 3-mercapto-1-propanol (MPrOH) affects the rate of viologen reduction during the assay of H184G. In the absence of thiol, the steady-state turnover results in a linear change in absorbance against time (dashed line). When 2 mM MPrOH is added to the cuvette just before the assay is started, the absorbance change slows down over the course of minutes, until the enzyme becomes inactive. No such effect was observed with the WT and H184C enzymes (data not shown).

Chronoamperometry. The activation and inhibition of H184G could be studied with the enzyme adsorbed on an electrode, in a configuration where electron transfer is direct (no mediator is used) and the turnover rate is simply measured as a current.[3,38,41,42] Figure 5 shows the change in activity against time, measured in such configuration, under 1 atm. of H_2, the electrode potential being poised at −160 mV vs SHE,[43] and following the addition to the electrochemical cell of 10 mM imidazole, then 2 mM 1-propanol (PrOH) and finally 2 mM MPrOH. The plain line in Figure 5 shows that the addition of imidazole results in an instantaneous activation, while MPrOH induces a slow decrease in activity against time, which mirrors the behavior in the H_2/MV assay (Figure 4). The fact that no change in activity is observed when PrOH is added (at $t = 150$s in Figure 5) proves that the inhibition results from the thiol group of 3-mercapto-1-pronanol. Under the same conditions, none of these molecules affects the activity of the WT enzyme (dashed line in Figure 5).

All the control experiments demonstrate that the exogenous ligands bind to the Fe atom whose coordination shell is incomplete in H184G.

Using Protein Film Voltammetry (PFV) to Probe the Competition between Inter- and Intramolecular ET. The experiments in Figure 5 confirm the previous observations regarding the effects of imidazole and thiol on the activity of H184G, but they do not reveal immediately the reason the activity varies upon ligand binding. We shall demonstrate that this information can be gained from voltammetry experiments, where the activity is measured over a wide range of driving force by sweeping the potential E of the electrode onto which the enzyme is adsorbed.

Figure 6 shows the voltammetric signature of the WT enzyme adsorbed at a rotating graphite electrode.[38] The voltammogram

(40) Dole, F.; Medina, M.; More, C.; Cammack, R.; Bertrand, P.; Guigliarelli, B. *Biochemistry* **1996**, *35*, 16399−16406.
(41) Léger, C.; Elliott, S. J.; Hoke, K. R.; Jeuken, L. J. C.; Jones, A. K.; Armstrong, F. A. *Biochemistry* **2003**, *42*, 8653−8662.
(42) Armstrong, F. A. *Curr. Op. Chem. Biol.* **2005**, *9*, 110−117.
(43) Under these conditions, hydrogen is oxidized by the enzyme, but the active site is not oxidized to one of its inactive states. See refs 38 and 44.

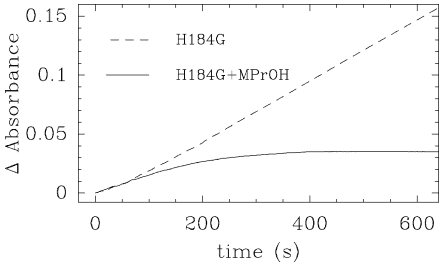

Figure 4. Inhibition of H184G by an alkane thiol: change in absorbance against time resulting from methyl viologen reduction by H184G in the absence (dashed line) or presence (plain line) of 3-mercapto-1-propanol (2 mM). pH 8, 30 °C, 1 atm of H_2.

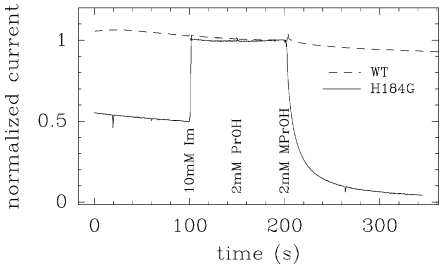

Figure 5. Activation and inhibition of H184G. The activity was measured as a current with the enzyme adsorbed onto a graphite electrode poised at −160 mV. The current was normalized to its value just before the thiol was added in the electrochemical cell. Effect of the addition of imidazole (at time $t = 100$ s), 1-propanol ($t = 150$ s) and 3-mercapto-1-propanol ($t = 200$ s) on the activity of H184G (plain line) and WT hydrogenase (dashed line). pH 7, 40 °C, 1 atm. of H_2, electrode rotation rate 2 krpm.

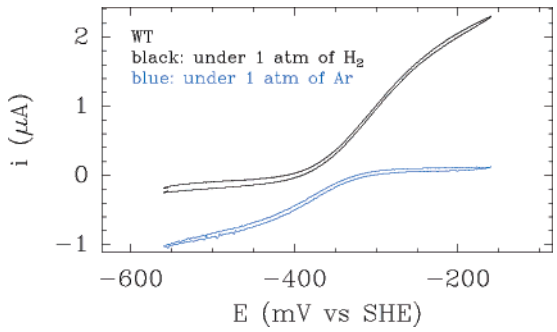

Figure 6. Voltammograms for WT *Df* NiFe hydrogenases adsorbed at a graphite electrode, under an atmosphere of H_2 (upper, black trace) or Ar (lower, blue trace), pH 7, scan rate $\nu = 10$ mV/s, electrode rotation rate $\omega = 1$ krpm, $T = 40$ °C.

plotted with a blue line has been recorded under an atmosphere of Ar, and the negative current at low potential results from proton reduction by the enzyme. The potential was swept slowly from −150 mV vs SHE down to −550 mV and back, and the fact that the signal is independent of the scan direction (except for the current offset that is due to double layer charging) implies that catalysis takes place at steady-state. Under an atmosphere of H_2, a positive current (upper, black line in Figure 6) reveals the oxidative activity at high electrode potential.

The theory that applies to the direct, catalytic electrochemistry of enzymes was developed and applied to several systems in recent years (refs 16, 42, 45, and refs therein). Here, we only recall the simple rules that allow the semiquantitative interpretation of the electrochemical experiments we shall report. In Figure 7, we decompose the catalytic cycle of NiFe hydrogenase into two parts: (i) interfacial ET steps, leading to the oxidation or reduction of the surface exposed [4Fe4S] cluster and (ii) the rest of the cycle, described by a pseudo-first-order rate constant

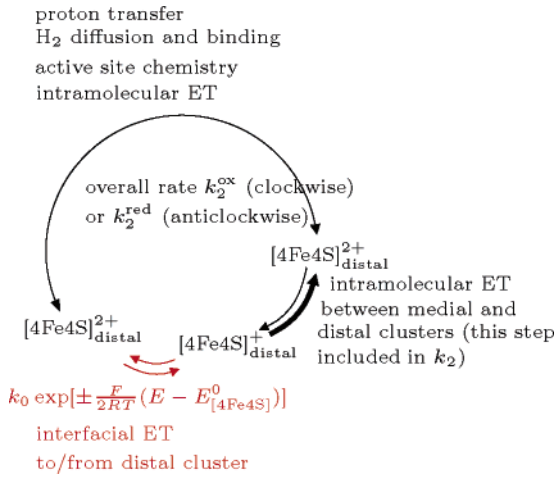

Figure 7. Minimal catalytic cycle for H_2 oxidation or production by NiFe hydrogenases adsorbed onto an electrode. We note E the electrode potential.

k_2 (with subscript "ox" or "red" for H_2 oxidation or production, respectively), which incorporates intramolecular ET along the chain of FeS clusters, H_2 diffusion and binding, active site chemistry and proton transfers. The rate of interfacial ET is proportional to a parameter called k_0 and depends exponentially on the electrode potential E, whereas k_2 is independent of E. How the catalytic waveshape depends on k_2 and k_0 is discussed in ref 46 and illustrated in the Supporting Information: at high driving force (high electrode potential for a catalytic oxidation, low E for reductive catalysis), the current changes linearly with E, with a slope that is proportional to k_2 and independent of k_0, whereas the shape of the wave is highly dependent on the ratio k_2/k_0, fast interfacial ET with respect to chemistry making the wave more sigmoidal.

Therefore, whether the change in coordination of the distal cluster in NiFe hydrogenase affects interfacial or intramolecular ET is expected to reflect differently on the shape (as opposed to merely the magnitude) of the catalytic voltammogram and this makes PFV superior to homogeneous kinetics, where the steady-state activity is only a measure of the rate of the slowest step in the catalytic cycle.

Voltammetry: All-Sulfur Coordination Slows Interfacial ET. Figure 8A shows the voltammograms recorded with the H184G variant under the same conditions as for the WT enzyme in Figure 6, before (dashed lines) and after (plain lines) we added imidazole. The important observations are that (i) the glycine variant has a residual activity in the absence of imidazole, (ii) the magnitude of the signal increases upon addition of imidazole (this mirrors the chemical rescue of the enzyme in solution assays, Table 1 and Figure 3), and (iii) the shape and position of the voltammogram for the repaired enzyme are very similar to those for the WT.[47]

The behavior of the H184C enzyme in Panel B is completely different from that of the WT and H184G-imidazole adduct: in this case, there is a large window of electrode potential,

(44) Jones, A. K.; Lamle, S. E.; Pershad, H. R.; Vincent, K. A.; Albracht, S. P. J.; Armstrong, F. A. *J. Am. Chem. Soc.* **2003**, *125*, 8505−8514.
(45) Reda, T.; Hirst, J. *J. Phys. Chem. B* **2006**, *10*, 1394−1404.
(46) Léger, C.; Jones, A. K.; Albracht, S. P. J.; Armstrong, F. A. *J. Phys. Chem. B* **2002**, *106*, 13058−13063.
(47) The magnitude of the current in Figure 8A is smaller than that with the WT enzyme, but since it is proportional to the unknown amount of enzyme adsorbed onto the electrode, this observation does not demonstrate that the repaired enzyme has lower activity than the WT (even if we know from solution assays that this is so).

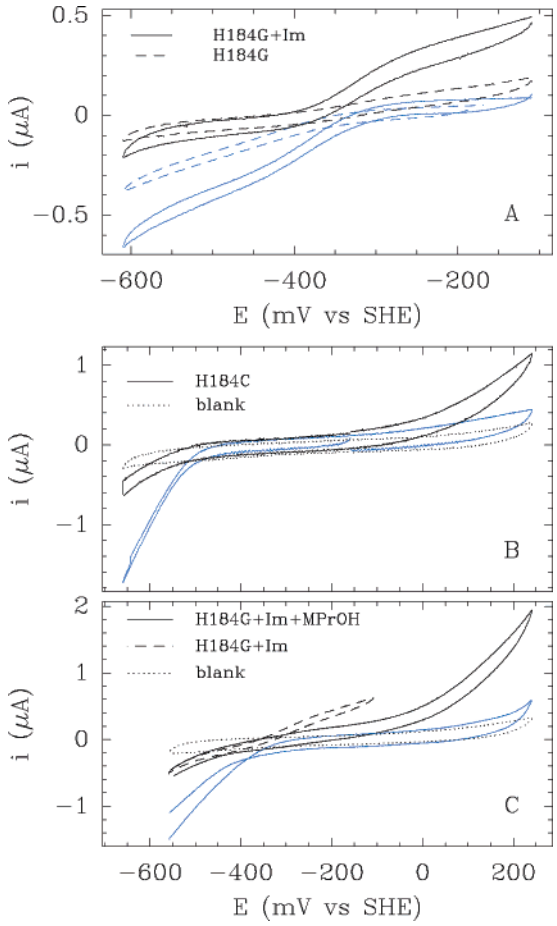

Figure 8. Voltammograms for the NiFe hydrogenases variants adsorbed at a graphite electrode, under an atmosphere of H_2 (black lines) or Ar (blue lines). Panel A: H184G mutant at pH 7, before (dashed lines) and after the addition of 20 mM imidazole. Panel B: H184C enzyme, at pH 6. Panel C: H184G mutant, at pH 6, in the presence of 10 mM imidazole, before (dashed line) and after the addition of 2 mM mercapto propanol (MPrOH). $\nu = 10$ mV/s, $\omega = 1$ krpm (Panel A) or $\nu = 20$ mV/s, $\omega = 2$ krpm (Panels B and C). $T = 40$ °C in all cases.

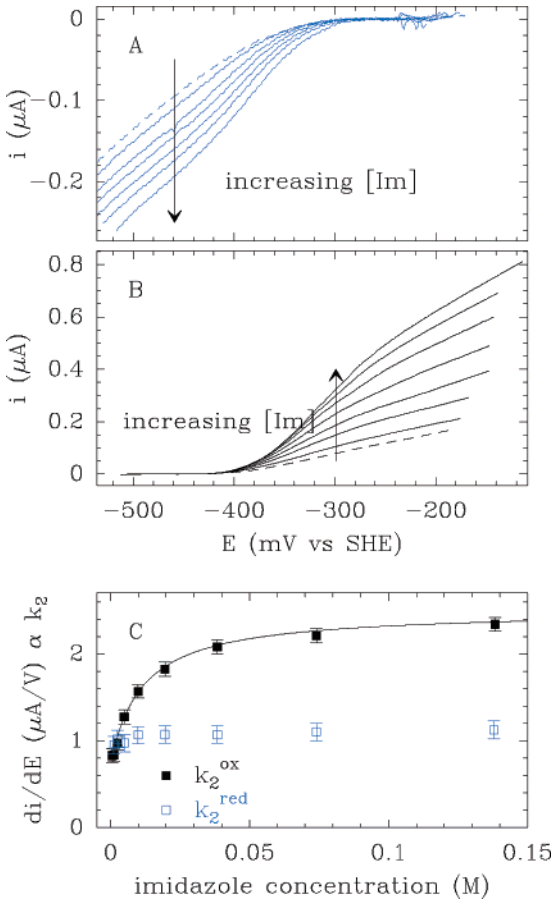

Figure 9. Effect of exogenous imidazole on the activity of *Df* H184G NiFe hydrogenase adsorbed at a graphite electrode. Panel A: H_2-production under 1 atm. of Ar. Panel B: H_2-oxidation under 1 atm. of H_2. The Panel C shows how the limiting slope of the voltammograms at high driving force (low potential for H^+ reduction, high potential for H_2 oxidation) changes as a function of the concentration of imidazole. The black line in Panel C is the best fit of k_2^{ox} to eq 1. pH 7, $T = 40$ °C, $\nu = 10$ mV/s, $\omega = 2$ krpm.

between −400 and −200 mV, where no activity is detected. The following observations confirm that the current at very low or very high *E* results from catalytic H_2 production or oxidation catalyzed by the H184C enzyme: (i) the signal is present only if the enzyme is adsorbed (the dotted line shows a blank recorded with no enzyme adsorbed on the electrode); (ii) the oxidation current (positive) disappears under an atmosphere of Ar (black line) and the reductive current decreases when the atmosphere is switched to H_2, which is known to inhibit H^+-reduction;[38,48] and (iii) we used the method described in ref 38 to check that the H^+ reduction current is reversibly inhibited by CO and H_2, and that the H_2-oxidation current is reversibly inhibited by CO and irreversibly inhibited by O_2, and the inhibition constants and rates of inactivation did not differ significantly from those measured for the WT (data not shown).

The shapes of the voltammograms for the H184C mutant reveal immediately sluggish interfacial electron transfer: only at very high driving force (either very low or very high electrode potential) is the rate of interfacial ET to or from the enzyme high enough to result in a turnover rate that can be distinguished from the background (compare with Figure S1 in the supplementary information).

Panel C shows the data for the H184G enzyme, repaired by imidazole (dashed line) and then irreversibly inhibited by adding 2 mM thiol in the cell (plain lines). It appears immediately that the binding of the thiol to H184G has the same effect as the His to Cys mutation: it slows interfacial ET.

Voltammetry: Effect of Imidazole Binding on Intramolecular ET in H184G. We now examine how the precise shape of the catalytic signal for the H184G variant is affected by exogenous imidazole. For the experiments in Figure 9, the electrode potential was cycled repeatedly to monitor the potential-dependence of the rate of H_2 oxidation or production. The concentration of imidazole was increased every other scan, and we checked that the signals increased only following the addition of imidazole: this implied that the change in activity as a function of time did not result from slow enzyme activation, inactivation or film desorption. The "as-recorded" data are show in the Supplementary Information (Figure S4), while we plot in Figure 9 the voltammograms corrected by subtracting baselines extrapolated linearly from the region of the voltammogram where there is no catalytic current.[46]

Figure 9A shows how the activity for proton reduction by H184G depends on the concentration of imidazole. Upon

(48) Léger, C.; Jones, A. K.; Roseboom, W.; Albracht, S. P. J.; Armstrong, F. A. *Biochemistry* **2002**, *41*, 15736−15746.

increasing the concentration, the waveshape changes from revealing sluggish interfacial ET (dashed line) to resembling that observed with the WT enzyme (compare with Figure 6); however, the slope of the signal measured in the high driving force limit remains unaffected (empty squares in Figure 9C). This change in shape shows that under reducing conditions, the binding of imidazole increases the rate of interfacial ET (through k_0) but has no effect on k_2^{red} (see the discussion above or compare with Figure S1, Supporting Information).

The data plotted in Figure 9B were recorded with the solution under an atmosphere of H_2, and the positive current reveals hydrogen oxidation by the enzyme. The magnitude of the current and the slope at high potential (filled squares in Panel C) both increase with increasing ligand concentration. The fit of the hyperbolic dependence of k_2^{ox} on the concentration of imidazole (eq 1 and black line in Figure 9C) gives a dissociation constant of 12 mM (at 40 °C, pH 7), in fair agreement with the value measured in solution (40 mM at pH 8, 30 °C). Such increase in slope of the catalytic data at high driving force is usually observed when an increase in k_2 results from the addition of substrate to the solution in contact with the adsorbed enzyme.[49,53]

Therefore imidazole binding increases k_0 and k_2^{ox}, but leaves k_2^{red} unchanged. The effect on interfacial ET (k_0) mirrors the chemical rescue of intermolecular ET in solution assays of the enzyme. The observation that k_2^{ox} increases upon imidazole binding to the distal cluster reveals an acceleration of intramolecular ET from the medial [3Fe4S] cluster to the distal cubane: all the other steps which may contribute to k_2^{ox} take place far from the distal cluster where imidazole binds and indeed, imidazole has no effect on the active site chemistry and proton transfers (as shown for all three enzymes by the experiments of isotope exchange and proton reduction in the presence of imidazole, Table 1).

In summary, imidazole-binding increases all rates of ET to or from the modified distal cluster, except the intramolecular, downhill step from distal to medial cluster in proton reduction, for which we detected no effect. The effect on intermolecular ET was revealed by traditional kinetics, while PFV was used here to demonstrate the effect on interfacial and intramolecular ET.

Discussion

In respiratory NiFe hydrogenases, a histidine ligates one Fe atom of the [4Fe4S] cluster that is remote from the active site and exposed at the surface of the protein (Figure 1). To understand the role of this residue, we have studied the effect of ligand substitution on the catalytic properties of the enzyme. The histidine was changed into a cysteine, to engineer a canonic, all-cysteinyl ligation, or into a glycine, to induce the formation of a [4Fe4S] cluster with a labile and exchangeable ligand. The essential role of the histidine ligand is demonstrated by the fact that the activities of the variants are only a few percent of that of the WT enzyme in the assays of H_2 oxidation with either MB or MV as electron partner.

Our spectroscopic results indicate that a [4Fe4S] distal cluster is assembled in both variants: (i) the elemental analyses show that a distal clusters is present, (ii) the EPR signatures of the oxidized variants in Figure 2A rule out the presence of a second [3Fe4S] cluster in either mutant (clearly, there has been no cluster conversion), and (iii) the EPR spectra of the reduced enzymes in Figure 2C show patterns of interaction between the reduced clusters that are similar to that for the WT enzyme. We expected the deletion of the imidazole ring of H184 in the glycine variant to open a gap in the coordination shell of an Fe that belongs to the distal cubane, and to make it amenable to direct manipulation through the addition of exogenous ligands. Indeed, we have used the results of activity measurements in the presence of imidazole derivatives and alkane thiols to bring further evidence of the existence of a distal [4Fe4S] cluster in H184G and to investigate how the coordination of the cluster affects the activity of the enzyme. The control experiments we report show that these ligands have no effect on the activity of the WT and H184C enzymes, both in solution assays (Table 1) and when the activity is measured with the enzyme adsorbed at an electrode surface (Figure 5), whereas they affect strongly the activity of the H184G enzyme. This demonstrates that these ligands bind to the cluster that is modified by the glycine mutation, most likely to the exposed Fe atom either free or bound to a labile solvent molecule, as already observed in other FeS-containing proteins. Armstrong and co-workers used PFV to demonstrate that a thiolate (2-mercapto-ethanol) binds to the unique iron of the $Asp(Cys)_3$-ligated $[4Fe4S]^{2+}$ cluster of *D. africanus* 8Fe ferredoxin.[54] In the case of a hydrogenase maturation protein that houses a [4Fe4S] cluster with only three proteic ligands, the binding of exogenous imidazole to the cluster's fourth Fe atom was demonstrated using HYSCORE spectroscopy.[55] Such detailed spectroscopic study of the distal cluster in H184G is precluded by the strong inter cluster spin−spin coupling which results in a broad EPR spectrum in the reduced state.

The activity of the H184G variant is intermediate between those of the WT and H184C enzymes, and it can be turned up or down upon binding of imidazole or thiol, respectively (Figures 3−5). It is also significant that these external ligands transform the electrochemical fingerprint of the H184G enzyme into that of the WT or H184C enzymes (Figures 6 and 8). This demonstrates that the exogenous ligands can substitute, to some extent, for the cluster's proteic ligand that is missing in the H184G enzymes. However, our kinetic data also point out the importance of the attachment of the ligand to the protein backbone. Indeed, the H184G-thiol adduct has no detectable oxidative activity in solution assays (whereas the activity of

(49) This was reported in the literature with arsenite oxidase in ref 50, Figure 7; sulfite oxidase in ref 51, Figure 5; lactate dehydrogenase in ref 16, Figure 2; Complex I in ref 45, Figure 5; nitrite reductase in ref 52, Figure 3 and hydrogenase in ref 48, Figure 2.

(50) Hoke, K. R.; Cobb, N.; Armstrong, F. A.; Hille, R. *Biochemistry* **2004**, *43*, 1667−1674.

(51) Ferapontova, E. E.; Ruzgas, T.; Gorton, L. *Anal. Chem.* **2003**, *75*, 4841−4850.

(52) Angove, H. C.; Cole, J. A.; Richardson, D. J.; Butt, J. N. *J. Biol. Chem.* **2002**, *277*, 23374−23381.

(53) In H_2 oxidation by H184G, Figure 9B, imidazole binding does not only increase k_2^{ox}: the similar effect on k_0 is suggested by the fact that the wave does not become less sigmoidal as the concentration of ligand is increased, as would be observed if the ratio k_2^{ox}/k_0 increased (compare Figure 9B to Figure 1 in ref 46 or Figure 2 in ref 48, or to Figures S2 and S3 in the Supporting Information). This was expected because in discussing Figure 9A, we have shown that imidazole binding increases k_0 when the enzyme reduces protons, and the rate of interfacial ET is proportional to k_0 regardless of the direction of electron flow.

(54) Butt, J. N.; Sucheta, A.; Armstrong, F. A.; Breton, J.; Thomson, A. J.; Hatchikian, E. C. *J. Am. Chem. Soc.* **1993**, *115*, 1413−1421.

(55) Brazzolotto, X.; Rubach, J. K.; Gaillard, J.; Ganbarelli, S.; Atta, M.; Fontecave, M. *J. Biol. Chem.* **2006**, *281*, 769−774.

H184C is 1.7% of that of the WT) and the chemical rescue of H184G by exogenous ligands is incomplete: none of the molecules we tested[56] could make the mutant recover more than 30% of the oxidative activity of the WT enzyme.

Effect of the Mutations on the Expression and Stability of the Proteins. Exchanging a direct ligand of a [4Fe4S] cluster is often destabilizing enough to impair cluster assembly or even protein folding (this was comprehensively reviewed by Moulis[29]). In this respect, it is striking that in the case of the H184G variant of *Df* NiFe hydrogenase, the protein is actually properly folded but the purification yield is 2 orders of magnitude lower than for the WT: this mutant would certainly have escaped detection if we had not used an affinity purification procedure. The purification yield of the H184C variant was similar to that for the WT, suggesting that the absence of the fourth proteic ligand in H184G slows down the folding of the protein and makes the nascent polypeptide prone to degradation by the expression host. However the mutations did not appear to decrease the "shelf life" of the purified proteins, which could be handled with no special care without loss of activity over time.

Mutations Impair Intermolecular ET. We have shown that mutating the histidine ligand of the distal cubane impairs neither cofactor incorporation nor protein folding, and has no effect on the structural and electronic properties of the NiFe active site (the EPR signatures of the active site states are unaffected by the mutations). Since we do not know the dissociation constant between the mutants and the physiological electron partner cytochrome c_3, we should not exclude a role of the histidine in partner recognition. However, we have shown that changing the ligation of the distal cluster has a strong effect on the *maximal* rate of H_2 oxidation (extrapolated to infinite concentrations of MV). These maximal rates eliminate effects of binding: they only incorporate contributions from first-order inter- and intramolecular ET, proton transfer and hydrogen activation at the active site. The mutations have no effect on the latter, since the enzymes retain their H^+/D_2 exchange activity (Table 1), and we also exclude the involvement of the $N_{\epsilon 2}$ of H184 in mediating a proton transfer step crucial for catalysis: were this to be the case, 1-methyl-imidazole could not rescue the H184G variant. Therefore, we conclude that the mutations impair electron transfer. Consistent with our earlier finding that proton-transfer limits reductive turnover,[22] the fact that the mutations have no significant effect on the rate of proton reduction demonstrates that the distal cluster is not directly involved in the rate-determining step for this reaction.

Considering the H_2-oxidation reaction, the fact that the activity is dependent on which electron acceptor is used shows that *intermolecular* ET limits oxidative turnover in the WT enzymes[3,22−24] and also in the variants. Thus, although ligand substitution may have an effect on both intra- and intermolecular ET, only the rate of the latter is probed in solution assays of H_2 oxidation: the decrease in rate of H_2 oxidation in Table 1 simply reveals the fact that the mutations slow ET to the soluble acceptor.

Mutations Slow Interfacial ET. We have used protein film voltammetry[41,42] to study the effects of the mutation or repair. In this technique, no soluble redox partner is used: the enzyme is simply adsorbed onto an electrode whose potential can be set to provide whichever driving force is required to sustain catalysis, and the steady-state activity is measured as a curve of current against electrode potential (E). The reason this technique proved useful is that the shape of the catalytic signal reveals the competition between the two processes that lead to the oxidation and reduction of the distal cluster during catalysis: intramolecular and interfacial ET.

The electrochemical results in Figure 8 provide an immediate demonstration of the detrimental effect of the all-sulfur coordination on interfacial ET in both the H184C mutant and in the thiol-inhibited H184G variant. The experiments in Figure 9 also show that imidazole binding to H184G increases the rate of interfacial ET. These effects on k_0 strongly supports the idea that impaired intermolecular ET is the reason these enzymes have so low activity in solution assays.

Intramolecular ET is Slow in H184G. When the electrons produced upon H_2 oxidation at the active site flow toward the electrode, the effect of imidazole is to increase the parameter k_0, that describes interfacial ET, but more surprisingly, it also increases the rate constant k_2^{ox} defined in Figure 7, and this has two implications: (i) the imidazole moiety increases the rate of intramolecular ET from the medial to the distal cluster, and (ii) in H184G, this step is slow enough with respect to the active site chemistry, proton transfer and H_2 diffusion, that it is rate determining when the enzyme is adsorbed at an electrode surface. This is in contrast with the general idea[17,18] that ET between closely spaced ($<$14 Å) redox centers is necessarily faster than the catalytic turnover. The distance between the medial and distal clusters is 8.5 Å in the WT enzyme, and the fact that the distal cubane in H184G remains attached to the structured protein by three buried cystein ligands makes very unlikely the hypothesis that it has moved away from the medial cluster; this hypothesis would also be very difficult to reconcile with the experiments of chemical rescue of the H184G variant by exogenous imidazole.

Why are ET Steps Slow in the Mutants? According to Marcus theory,[57] the rate of ET between the distal cluster and its redox partner (depending on which step we consider, this can be the electrode, the soluble dye, or the medial cluster) can be affected by a change in any of the following three parameters: (i) the reduction potential of the cluster, (ii) the electronic coupling between the cluster and the partner, and (iii) the reorganization energy of the process.

(i) Regarding intermolecular ET, we can exclude for both mutants that slow intermolecular ET toward the soluble acceptor (during H_2 oxidation) results from a mutation-induced *increase* in reduction potential of the distal [4Fe4S] cluster. In the case of H184C, this would be inconsistent with the results of our potentiometric titration which shows that the mutation may induce a small decrease in reduction potential but not a positive shift. For H184G, if the reduction potential of the distal cluster were greater than in the WT, this would speed intramolecular ET to the distal cluster, whereas the opposite, detrimental effect is demonstrated by our electrochemical study.

(ii) The low activity of both variants and the chemical rescue of H184G by imidazole[56] may reveal a function of the π bonds of H184 in increasing the electronic coupling between the distal

(56) The oxidative activity of the H184G variant is also partially rescued by exogenous pyrazole, triazole, pyridine and 4-ethyl-pyridine, while under identical conditions, these molecules have no effect on the WT and H184C enzymes (data not shown).

(57) Marcus, R. A.; Sutin, N. *BBA* **1985**, *811*, 265−322.

cluster and its partners. This could result from the change of coordination either modifying the valence localization pattern within the $[4Fe4S]^{+}$cluster, or altering the electronic pathway provided by the network of chemical bonds.

(iii) Last, the decrease in rate of ET to/from the distal cluster in the mutants may result from an increase in reorganization energy of the distal cluster. This effect is documented in the case of azurin[58] and copper-containing nitrite reductase,[59] which both house a surface-exposed, type-I copper site involved in ET: when a histidine ligand of the copper is mutated into a glycine, the cluster has much higher reduction potential and increased reorganization energy. The "redox-inactive" mutants exhibit extremely slow interfacial[58] or intermolecular[59] ET rates, unless repaired by exogenous imidazole. A significant increase of the value of λ in H184G compared to the WT enzyme would not be surprising considering how solvent exposure should affect the outer-sphere reorganization energy. It may also happen that the binding and dissociation of the exogenous ligand on the time scale of turnover has a considerable retarding influence. An increase in λ would have exactly the effect we observe in H184G: slowing down all ET rates to and from the cluster (intramolecular, intermolecular, and interfacial).

Considering specifically intramolecular ET, we note that the slow step in H184G (from the medial to the distal cluster) is the step that is very endergonic in the WT enzyme.[18,20] Therefore, unfavorable thermodynamics is likely to add to the effects of the mutation to slow this transfer. Consistently, we did not detect an acceleration of the reverse step (from the distal to the medial cluster) upon imidazole binding to H184G: this step is driven by such large driving force that it is not expected to be rate determining in proton reduction.

Overall, the fact that the mutations slow ET steps is unlikely to result from a change in reduction potential of the distal cluster; instead, the contributions of electronic coupling and reorganization energy must be considered.

(58) Jeuken, L. J. C.; van Vliet, P.; Verbeet, M. P.; Camba, R.; McEvoy, J.; Armstrong, F.; Canters, G. *J. Am. Chem. Soc.* **2000**, *122*, 12186−12194.
(59) Wijma, H. J.; Boulanger, M. J.; Molon, A.; Fittipaldi, M.; Huber, M.; Murphy, M. E. P.; Verbeet, M. P.; Canters, G. W. *Biochemistry* **2003**, *42*, 4075−4083.

Conclusions

Our results suggest that the short distance between FeS clusters in biological redox chains may not always be sufficient to allow rapid intramolecular ET: for very endergonic steps, other structural features, such as the distal cluster's ligation in NiFe hydrogenase, may have an essential yet undervalued function in making up for the unfavorable thermodynamics.

Whether or not intramolecular ET is also slower than hydrogen activation in the WT enzyme is still unknown and this reminds us that measurements of intramolecular ET rates are difficult and scarce in non-light-driven systems. We have shown recently that the detailed analysis of the shape of the voltammograms obtained for enzymes confined at an electrode surface could give quantitative information in this respect.[16] We are now using this approach to probe the efficacy of ET in WT *Df* NiFe hydrogenases, and in variants (including H184G, H184C, and P238C) where the ET chain is significantly modified.

Acknowledgment. We thank C. Hatchikian (BIP, Marseilles) for preparing the untagged *Df* NiFe hydrogenase, Alejandro Ballesteros (CSIC, Madrid) for technical assistance, P. Gallice and F. Chaspoul (Université de la Méditerranée, Dept. of Pharmacy, Marseilles) for carrying out the ICP-MS measurements and K. Meffrou (RMH, London) and F. Baymann (BIP, Marseilles) for fruitful discussions. This work was supported by the French CNRS, the University of Provence, the City of Marseilles, the Spanish MCYT (Project BQU2000-0991) and by the Grant G5RD-CT-2002-00750 from the European Union in the Competitive and Sustainable Growth Program.

Supporting Information Available: Simulations illustrating how k_2 and k_0 affect the shapes of the voltammograms. Uncorrected data for Figure 9. This material is available free of charge via the Internet http://pubs.acs.org.

JA060233B